TELEMETRY OF THE COCKCROFT-WALTON ACCELERATOR

by

JACK ROSS CRUMRINE

B. S., Kansas State University, 1969

A MASTER'S REPORT

submitted in partial fulfillment of the

requirements for the degree

MASTER OF SCIENCE

Department of Electrical Engineering

KANSAS STATE UNIVERSITY
Manhattan, Kansas

1971

Approved by:

Dale E. Hawkinson

Major Professor

TABLE OF CONTENTS

LIST OF ILLUSTRATIONS

CHAPTER I

INTRODUCTION

The essential object of a telemetry system is to gather data, translate it into a form suitable for transmission, transmit it to a remote location, and then display the data in a form useful for human interpretation. The location to which the display of data is delivered may be several feet or several thousands of miles from the source of information, depending on the physical barriers separating the transmitter and receiver. Thus, any telemetry system consists of three groups of equipment: a transmitter, a transmission medium, and a receiver or display unit.

In any system where an electrical analog of a measured variable is transmitted, two, rather than just one, measurements must be made; correspondingly, the possibility for introduction of error into the display image of the variable is doubled. These measurements take place at the location of the sensor (the original measurement) and at the display unit. There are also varying conditions of the data link or transmission medium which may cause errors in transmission. Thus, action should be taken to eliminate or lessen parameter variations in the transmitter, transmission medium, and receiver, in order to achieve a reasonable accuracy in data transmission.

Remote measurement schemes can take two general forms, digital or analog. In the digital case the transmitted image or measurand can assume one of a finite number of values owing to the analog to digital conversion techniques. The primary measurement is encoded into a digital format and must be

processed again prior to display. Thus, the transmitted information is a number. For the analog system, the transmitted image can assume an infinite number of values. In the analog system some parameter of the transmitted signal is directly analogous to the measurand. Strictly speaking, this includes certain pulse systems, for example, pulse amplitude modulation (PAM) and pulse position modulation (PPM).

CHAPTER II

THE PRESENT COCKCROFT-WALTON ACCELERATOR TELEMETRY SYSTEM

The Telemetry Problem

Each of the preceding facts concerning telemetry is of importance in the Cockcroft-Walton Accelerator. Figure 1 gives an idea of the present telemetry system.

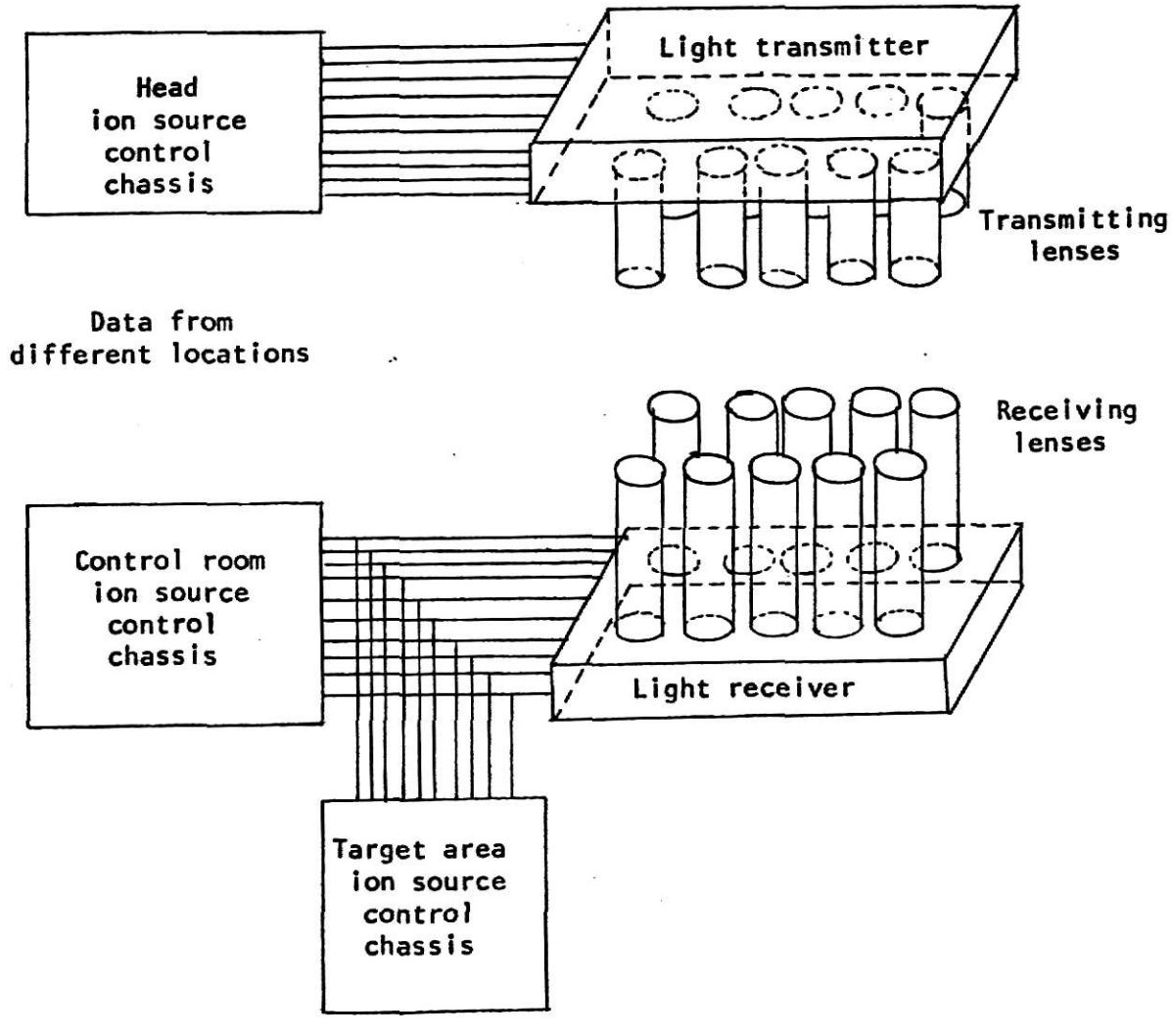

Fig. 1.--The present system

The Head Ion Source Control chasis and light transmitter are located in the high voltage area of the accelerator. All parameters of interest are located in the head and are transmitted to the receiving unit which is at ground potential, a distance of six feet. During normal operation the head voltage is 600 KV, necessitating a wireless telemetry system. The system which is presently operating was used at Los Alamos and will be briefly discussed before an improved version is proposed in this paper.

The Present Method

The original system was designed to transmit ten channels of data. Only four of these will be of interest in the new telemetry system: (1) Cage AC voltage, (2) focus voltage, (3) Anode current, (4) Filament current. Figure 2 is a diagram of the ion source with the last three of these four data sources labeled.

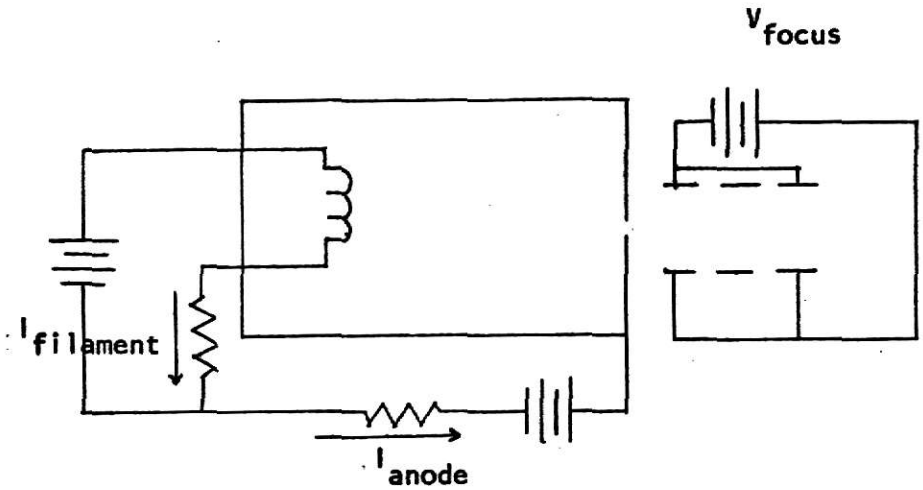

Fig. 2.--Ion Source

The system used for transmitting the data employed an analog technique. Argon bulbs were used in a simple relaxation oscillator to convert a d-c voltage to a controlled frequency for light transmission.

The pulsed light output from the relaxation oscillator is transmitted to a photomultiplier chasis located at the base of the accelerator. An intricate lens system is used to focus the pulsed light from the transmitter onto the photomultiplier tubes. Any slight misalignment of the lens system results in absolutely no transmission.

The receiving unit consists of a photomultiplier tube which amplifies the light pulses received from the argon bulb transmitter. These pulses are averaged over time and give a linear frequency to voltage conversion in the decoding circuit. The only requirement for linear frequency to voltage conversion is that the light output of the argon bulb remain high enough to drive the photomultiplier tubes. After proper lens alignment the major error in this system will be the voltage to frequency conversion technique using the argon bulbs.

Problems of the Voltage to Frequency Conversion Technique

Figure 3 shows a typical argon bulb relaxation oscillator.

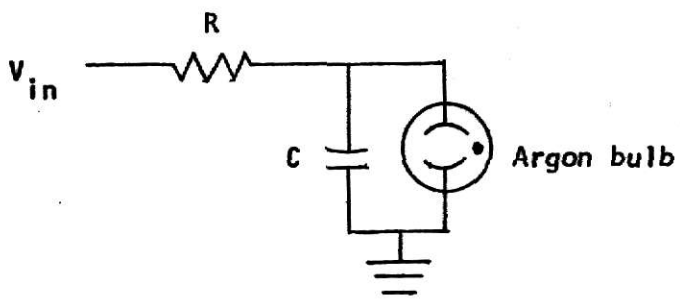

Fig. 3.--Relaxation Oscillator

When V_{in} is applied the voltage across the lamp is initially zero since the capacitor is not able to change its voltage instantaneously. The capacitor begins to charge to V_{in} with a time constant $\tau = RC$. Since the lamp is

in the non-conducting state at this time, the resistance of the lamp is so large that its shunting effect is usually negligible.

When the increasing voltage across the lamp reaches the dynamic breakdown voltage V_f, the lamp switches into the conducting or light emitting state with the lamp current increasing to a relatively high value. The capacitor then begins to discharge toward ground through the resistance of the lamp. The dynamic lamp resistance in the conducting state is variable depending on the value of the current flowing in the lamp, initially having a value of a few thousand ohms. The capacitor thus quickly discharges so that the voltage across the lamp decreases rapidly until it reaches the dynamic extinguishing voltage V_e. The lamp then switches to the high-resistance state with the lamp ceasing to glow. With the glow lamp thus switched to the high resistance state, the capacitor again begins to charge toward the input voltage V_{in}. With each capacitor discharge through the lamp, the lamp emits a pulse of light.

During the time the capacitor is charging the equation for the voltage wave form is:

$$v(t) = V_e + (V_{in} - V_e)(1-e^{\frac{-t}{RC}}). \qquad 0 \leq t \leq T_c$$

At the time T_c, $v(t)$ is equal to V_f. Thus,

$$V_f = V_e + (V_{in} - V_e)(1-e^{\frac{-T_c}{RC}}).$$

Solving for T_c gives

$$T_c = RC \ln \frac{V_{in} - V_e}{V_{in} - V_f}$$

Assuming that the time for C to discharge to V_e is much less than T_c,

which is true for low frequency oscillations, the period of a single cycle is approximately T_c and the frequency is the inverse of the period.

$$f = \frac{1}{RC \ln\left(\frac{V_{in} - V_e}{V_{in} - V_f}\right)} \qquad (1)$$

This equation holds true for frequencies below 200 Hz. This voltage to frequency conversion technique suffers from the inverse log variation with V_{in}.

Physical Problems of Glow Lamps

Typical characteristics for Glow lamps show several disadvantages for use as voltage controlled oscillators. First, from the frequency equation (1) the frequency is a logarithmic function of V_{in}. Secondly, V_f varies with frequency as shown in Figure 4.

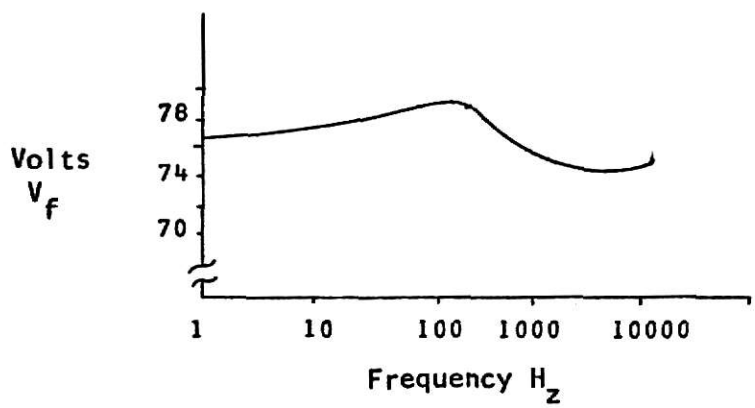

Fig. 4.--Frequency Variation of V_f

Figure 5 gives an indication of the variation of extinguishing voltage V_e with frequency.

These figures indicate the sources of errors in any simple voltage to

frequency conversion technique using argon lamps. Also the peak to peak signal amplitude $V_s = V_f - V_e$ varies with frequency; this is important in maintaining a constant amplitude light signal. Such variation is given in Figure 6.

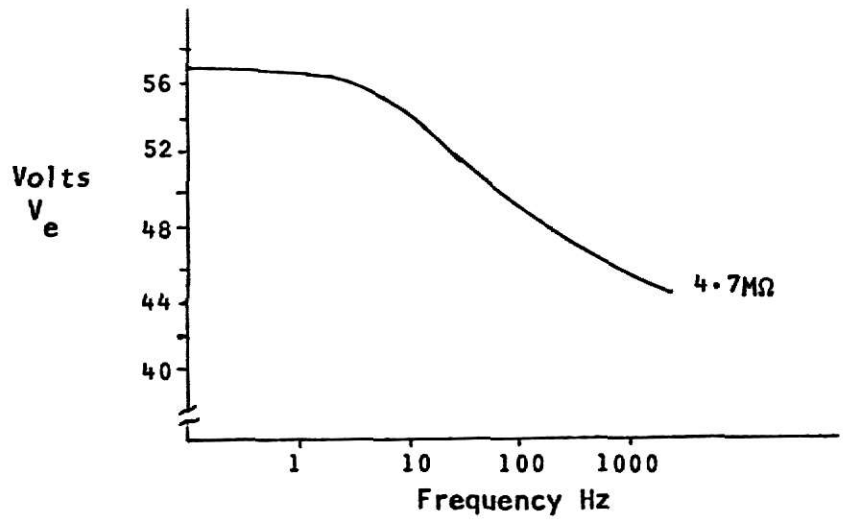

Fig. 5.--Frequency Variation of V_e

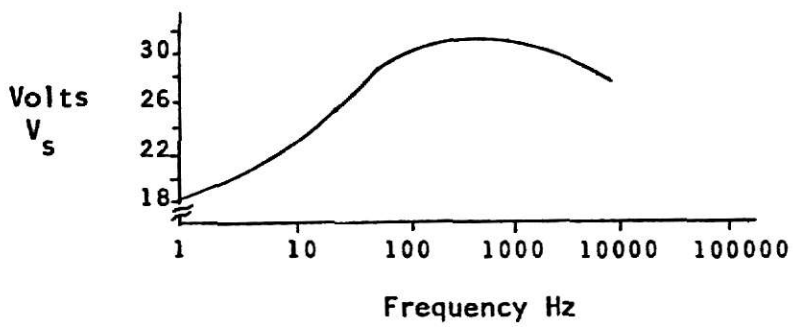

Fig. 6.--Frequency Variation of V_s

Another physical property of glow lamps is of interest; this is the effect of temperature on their operation. Any variation in frequency is essentially linear with temperature, but the degree and direction of change from the frequency at room temperature appears to be dependent upon the fre-

quency of operation. The rate of change in frequency with temperature may be as high as 1.5% of the frequency at room temperature per 10° C change in temperature.

When using glow tubes in relaxation oscillators, three types of frequency instability may be experienced:

a) Short term frequency instability which requires a length of time before the circuit has reached a steady frequency of operation. This occurs when the lamp is being used for the first time or after it has not been used for a period of time.

b) Gradual change in frequency with aging of the lamp.

c) Random changes in frequency of operation caused by a rapid change in lamp parameters.

These frequency instabilities are such that glow lamps operate very poorly as stable highly accurate voltage to frequency converters.

CHAPTER III

A PROPOSED TELEMETRY SYSTEM

The System in General

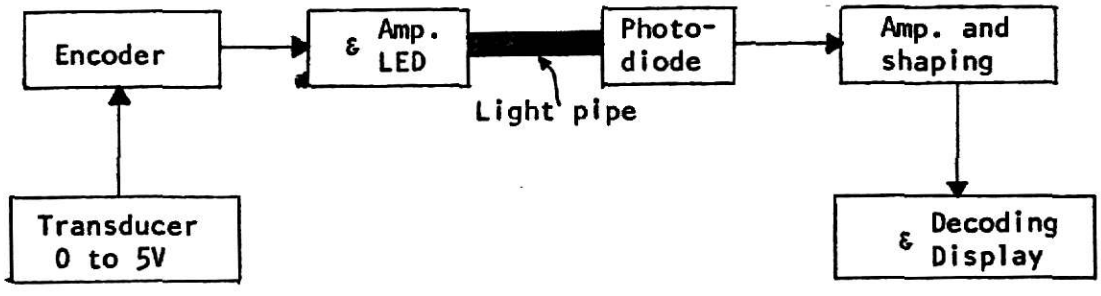

Fig. 7.--Block diagram of proposed system

The proposed telemetry system consists of an encoding circuit which is a multivibrator acting as a linear voltage to frequency converter, and driving a light emitting diode (LED). A lens system could be used for the transmitting channel; however, low cost plastic fiber optics capable of transmitting the wavelength of the LED will serve well as the transmitting channel. Also, by using fiber optics the alignment problem is essentially eliminated. The photodiode receives the light from the light pipe and produces a current proportional to the amplitude of the incident light. This signal is then amplified and shaped into a square wave which is then averaged to give a voltage proportional to the frequency of the transmitted signal.

Choosing the Encoder Circuit

Figure 8 is a typical astable multivibrator. Analysis of this circuit would give a constant value for the frequency of oscillation. However, by removing R_1 and R_2 from the supply V_{cc} and connecting them to an input voltage V_{in}, a simple voltage controlled oscillator as in Figure 9 is obtained.

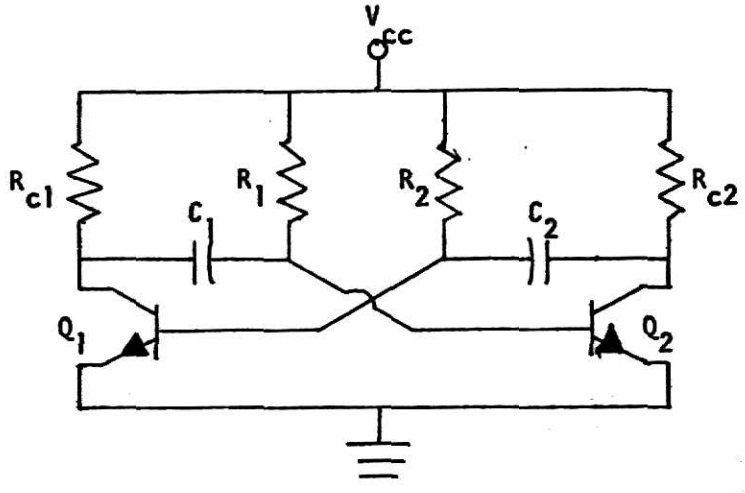

Fig. 8.--Astable multivibrator

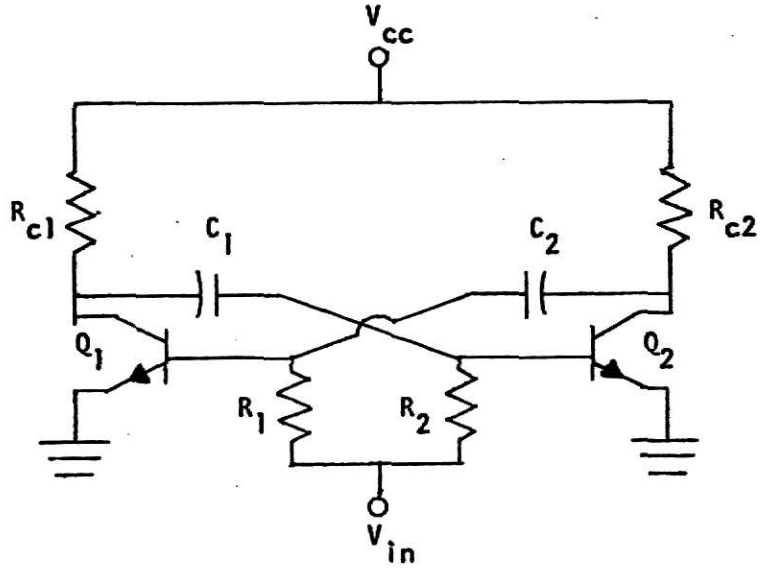

Fig. 9.--Simple voltage controlled oscillator

Consider Figure 10, where it is assumed transistor Q_1 is in saturation and its collector to emitter voltage is equal to $V_{ce} = 0$. The voltage V(t)

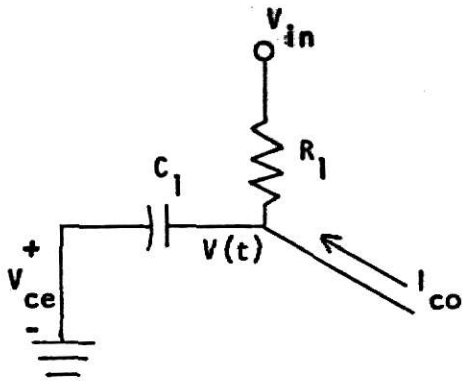

Fig. 10.--Quasi-stable state 1

at the base of transistor Q_2 during this quasi-stable state can be obtained from Figure 10. Using Kirchoff's current law:

$$C_1 \frac{d}{dt} V(t) + \frac{1}{R_1} [V(t) - V_{in}] - I_{co} = 0$$

or

$$V(t) + R_1 C_1 \frac{d}{dt} V(t) = I_{co} R_1 + V_{in} \tag{2}$$

Now applying the Laplace Transform to equation (2):

$$[1 + C_1 R_1 s] V(s) - C_1 R_1 v(0-) = \frac{1}{s} [V_{in} + I_{co} R_1] \tag{3}$$

where, $V(s)$ is the Laplace transform of $V(t)$
$V(0-)$ is the value of the voltage $V(t)$ at the instant of transition into the quasi-state of Figure 10 from the state indicated in Figure 11.

From Figure 11 the initial condition for $v(0-)$ is obtained. Transistor Q_2 is in saturation and its base voltage is equal to V_{be}, while transistor Q_1 is cutoff and its collector voltage is effectively V_{cc}. Immediately after transition to the state in Figure 10, Q_1 is driven into saturation and its collector voltage, therefore, falls to a value equal to $V_{ce} = 0$. Since the voltage across the capacitor cannot change instantaneously, it follows that the voltage at the base of transistor Q_2 must fall to $-V_{cc} + V_{ce} + V_{be}$ immediately after transition to the state in Figure 10. Thus,

$$v(0-) = -V_{cc} + V_{ce} + V_{be}. \tag{4}$$

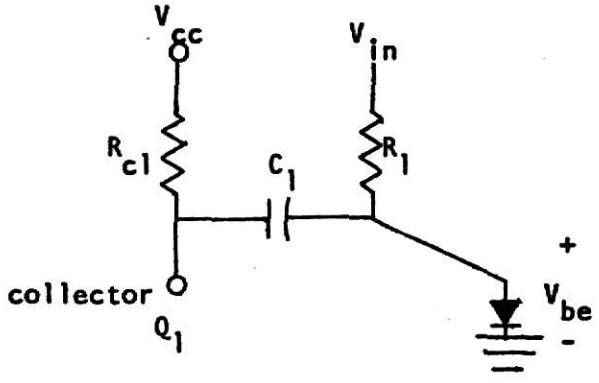

Fig. 11.--Quasi-stable state 2

Equations (3) and (4) give

$$(1 + C_1R_1s)V(s) - C_1R_1(-V_{cc} + V_{ce} + V_{be}) - \frac{1}{s}(V_{in} + I_{co}R_1)$$

or,

$$V(s) = \frac{-V_{cc} + V_{ce} + V_{be}}{s + \frac{1}{R_1C_1}} + \frac{V_{in} + I_{co}R_1}{R_1C_1s(s + \frac{1}{R_1C_1})}.$$

Expanding V(s) in partial fractions yields

$$V(s) = -\left[\frac{V_{cc} + V_{in} - V_{ce} - V_{be} + I_{co}}{s + \frac{1}{R_1C_1}}\right] + \frac{1}{s}(V_{in} + I_{co}R_1).$$

Taking the inverse Laplace Transform yields:

$$V(t) = -(V_{cc} + V_{in} - V_{ce} - V_{be} + I_{co}R_1)\, e^{-\frac{t}{R_1C_1}} + (V_{in} + I_{co}R_1). \tag{5}$$

Figure 12 is the waveform of equation (5). Examination of Figure 12 indicates that the voltage V(t) at the base of transistor Q_2 rises from the value v(0-) up to a value V_γ at $t = \tau_0$, where V_γ is the base-emitter turnon voltage of Q_2.

It therefore follows that transistor Q_2 will remain cutoff for a period equal to τ_0 after which its base voltage becomes equal to V_{be} since the astable multivibrator has changed state. Hence, τ_0 is effectively equal to one half of the timing period of the symmetric astable when $R_1 = R_2 = R$ and $C_1 = C_2 = C$.

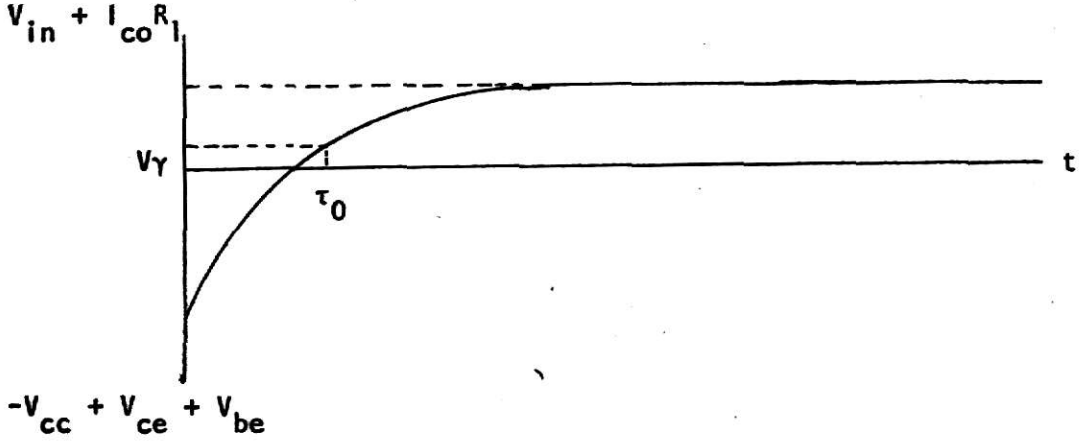

Fig. 12.--Waveform of equation (5)

The value of τ_0 is obtained from Figure 12 when $V(t) = V_\gamma = V_{be}$ at $t = \tau_0$. From equation (5) we obtain:

$$V_{be} = -(V_{cc} + V_{in} - V_{ce} - V_{be} + I_{co}R)e^{-\frac{\tau_0}{RC}} + V_{in} + I_{co}R$$

or,

$$\tau_0 = CR \ln \frac{V_{cc} + V_{in} - V_{ce} - V_{be} + I_{co}R}{V_{in} + I_{co}R - V_{be}}$$

Clearly, this circuit suffers from a logarithmic relationship as did the argon bulb relaxation oscillator. Assuming that $V_{ce} = 0$, $V_{in} >> V_{be}$, and $V_{in} >> I_{co}R$,

$$\tau_0 = CR \ln \left(1 + \frac{V_{cc}}{V_{in}}\right).$$

The frequency $f = \frac{1}{2\tau_0}$; thus

$$f = \frac{1}{2RC \ln \left[\frac{V_{in} + V_{cc}}{V_{in}} \right]} \tag{6}$$

To avoid this nonlinear voltage to frequency conversion the substitution of constant current sources for base resistors is necessary.

Figure 13 is the multivibrator of Figure 9 with constant current sources I substituted for the base resistors. The constant current sources will be a linear function of V_{in}, i.e., $I = k_1 V_{in} + k_2$.

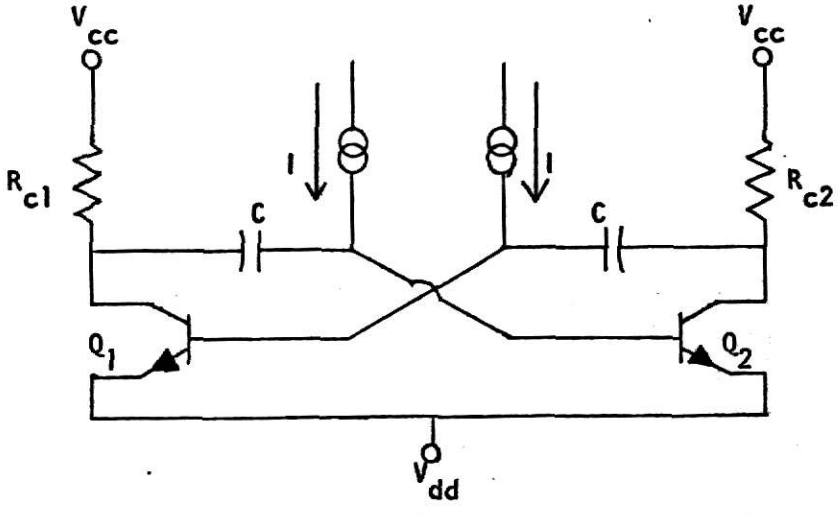

Fig. 13.--An improved voltage controlled oscillator

Once again for Figure 13 consider Q_1 in saturation so that its collector voltage relative to emitter is V_{ce}. The voltage V(t) at the base of transistor Q_2 can be obtained from Figure 14.

Writing Kirchoff's current law at the base of Q_2, we have:

$$C \frac{d}{dt} V(t) - I - I_{co} = 0. \tag{7}$$

Taking the Laplace Transform of (7) yields:

$$Cs\, V(s) - C\, v(0-) = (I + I_{co}) \frac{1}{s}. \tag{8}$$

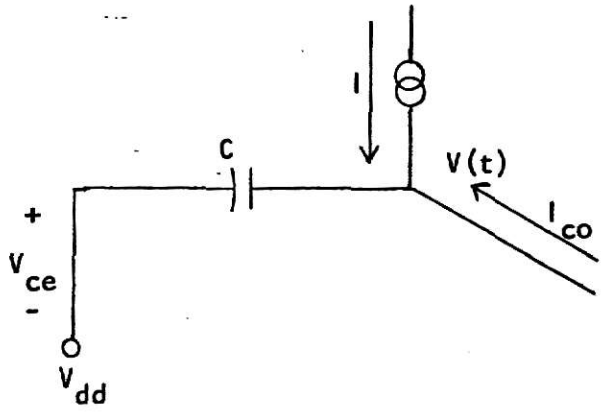

Fig. 14.--Quasi-stable state 1

Evaluating v(0-) using Figure 15 we have:

$$v(0-) = -(V_{cc} - V_{ce} - V_{dd}) + V_{be} + V_{dd}. \tag{9}$$

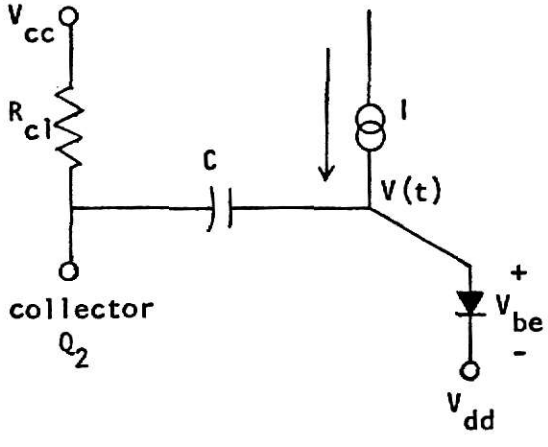

Fig. 15.--Quasi-stable state 2

Combining (8) and (9) produces

$$V(s) = \frac{(I + I_{co})}{s^2 C} + \frac{C}{sC}\,[2\,V_{dd} + V_{be} - V_{cc} + V_{ce}]. \tag{10}$$

The inverse Laplace Transform gives:

$$V(t) = \frac{I + I_{co}}{C} t + 2V_{dd} + V_{be} - V_{cc} + V_{ce} . \tag{11}$$

In this case at $t = \tau_0$ $V(t) = V_{be} + V_{dd}$ and (11) becomes

$$V_{be} + V_{dd} = \frac{I_{in} + I_{co}}{C} \tau_0 + 2 V_{dd} + V_{be} - V_{cc} + V_{ce}$$

or

$$\tau_0 = \frac{C}{I + I_{co}} [V_{cc} - V_{dd} + V_{ce}] .$$

The frequency $f = \frac{1}{2\tau_0}$ is of interest; therefore,

$$f = \frac{I + I_{co}}{2C[V_{cc} - V_{dd} + V_{ce}]} \tag{12}$$

Recall $I = k_1 V_{in} + k_2$ is the form of the constant current source; therefore, the desired linear voltage to frequency conversion is obtained.

The design of a constant current source which will give the desired result, i.e., a constant current that is linearly dependent on the input voltage is considered next. Figure 16 is such a circuit.

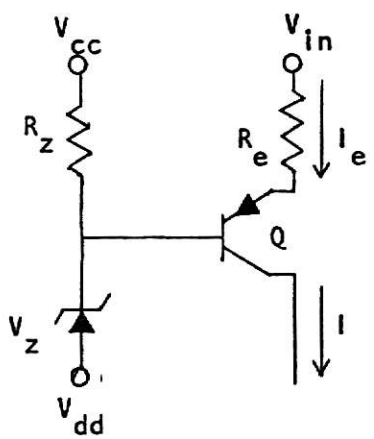

Fig. 16.--Constant current source

Analysis of this circuit gives:

$$I_e = \frac{V_{in} - V_z - V_{dd} + V_{be}}{R_e}$$

$$I = \alpha I_e + I_{co}$$

where α is the total forward current gain of the transistor as viewed from an external circuit $\alpha = \frac{I_c}{I_e}$.

Thus,

$$I = \frac{\alpha}{R_e} V_{in} + \frac{\alpha}{R_e} [V_{be} - V_z - V_{dd}] + I_{co}$$

or,

$$I = k_1 V_{in} - I_{co}. \tag{13}$$

Where

$$k_1 = \frac{\alpha}{R_e},$$

and V_{dd} has been adjusted to

$$V_{dd} = \frac{2R_e}{\alpha} I_{co} + V_{be} - V_z.$$

Combining (12) and (13),

$$f = \frac{k_1 V_{in}}{2C[V_{cc} - V_{dd} + V_{ce}]}. \tag{14}$$

This gives the linear voltage to frequency conversion as desired.

Practical Problems of the Encoder Circuit

The two major sources of difficulties are timing period stability and linearity errors. Timing period errors will be due to one or more of the following phenomena:

(a) Variation in the passive circuit components such as resistors and capacitors. These must be chosen correctly in order to give the required period stability since, in general, the timing period is proportional to capacitor C, and the resistor R_e in the constant current circuit.

(b) Variation in the supply voltages V_{cc} and V_{dd}.

(c) Variation in the parameters of the transistor.

A main source of variation is a change in the parameters of the transistor owing to the variations in ambient temperature or in loading. Also, I_{co} variation is a major cause of timing period variation when germanium transistors are used. The silicon transistor leakage currents are small enough to make such an effect negligible at temperatures up to 60° C. As long as the supply voltage is large compared to V_{be} the temperature variation of V_{be} will be negligible.

By using a stabilized power supply and silicon transistors, the stability problem becomes one of choosing resistors and capacitors with opposite thermal coefficients. It is feasible in a single design to choose transistors and components which will give a multivibrator with almost zero temperature coefficient. However, the process of component selection with this in mind is tedious when several circuits are to be built. Furthermore, the process must be repeated if components are replaced when faulty. Thus, silicon transistors, a stabilized power supply, and quality resistors and capacitors will be used.

Where accurate measurement of the period is required, errors may be introduced by the finite rise and fall times of the multivibrator waveform. The main defect of the collector waveform from a timing point of view is the degraded rise time, which is due to the flow of the capacitor charging current

in the collector load resistor. The waveform can be much improved by routing the charging current via resistors R_{d1} and R_{dz} and by the inclusion of diodes as shown in Figure 17. The collector waveform is shown in Figure 18 where

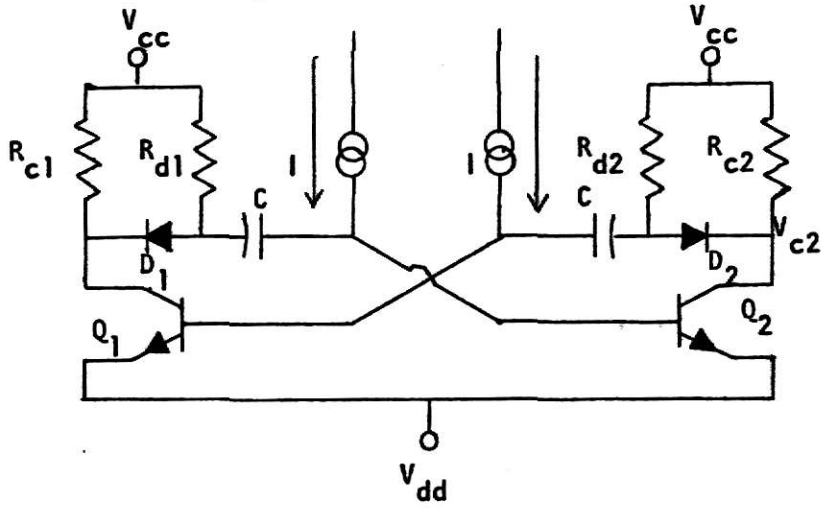

Fig. 17.--Multivibrator with diodes for collector waveform improvement

Fig. 18.--Waveforms at collector

with the diode in the circuit the charging current is isolated from the collector load; thus, the collector rise time is much shorter.

The Encoder Circuit

Figure 19 is the final multivibrator (encoder) circuit. This circuit requires an input voltage V_{in} of 5 volts to produce a 100 Hz output waveform. When V_{in} is zero the frequency should be zero, but the lowest attainable oscillation is 10 Hz at 0 volts.

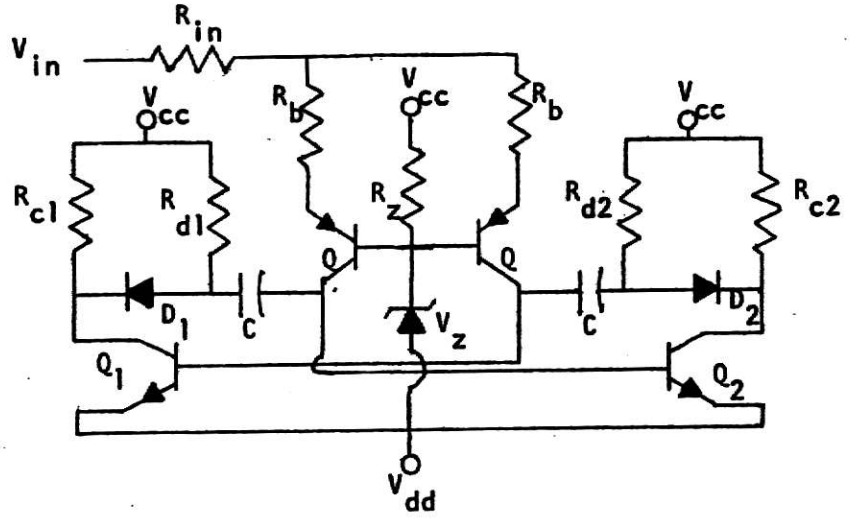

Fig. 19.--Encoder circuit

As mentioned in Chapter II, there are two currents to be measured; thus a stage of amplification will be necessary to change the 50 mv shunt voltage to a 5 volt input to the encoder circuit. Consider the filament circuit of Figure 20, where an operational amplifier (Op Amp) has been added across the ammeter shunt. The Op Amp used in this case is a μA 741. The circuit includes a zero adjust resistor R_0, which will yield an output of zero volts when there is no current flowing in the filament circuit. When the ammeter of the filament circuit is at 20 A. (or full scale), the ammeter shunt will have 50 mv. across it causing V_{in} to be a value of 5 volts as desired. This voltage, V_{in} is the input to the encoder of Figure 18. Resistor R_a is included

to have control over the gain in case 5 volts input to the encoder is not adequate.

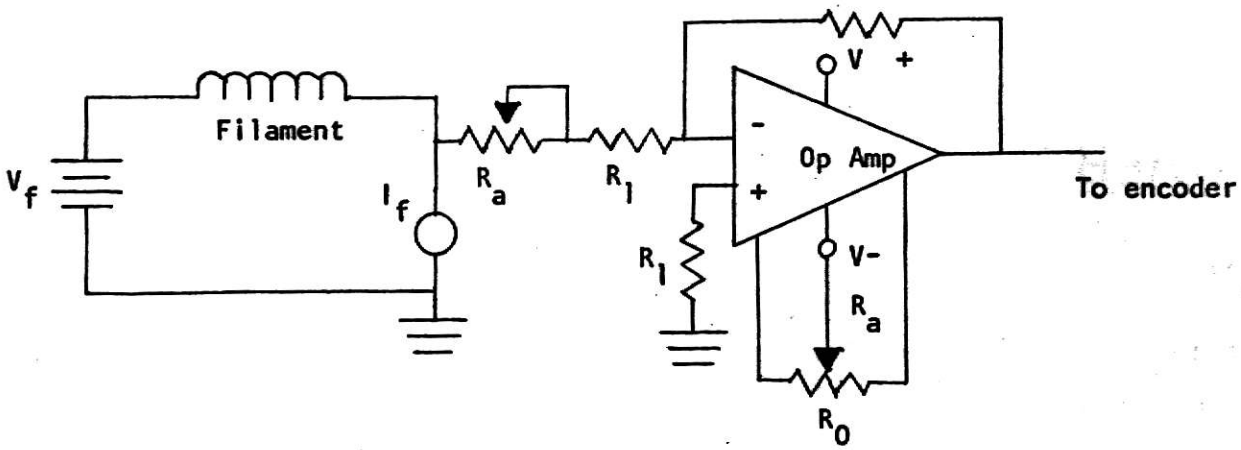

Fig. 20.--Amplifier circuit

The LED and Associated Circuitry

The encoded frequency will drive a LED which is optically coupled to the receiving unit where it will be decoded. Thus, the properties of the LED will be of importance in obtaining proper light transmission.

One of the important considerations in fitting a LED to a particular application is power dissipation; this is the limiting factor on the output of these devices. Figure 21 is a typical curve of a LED where point A is the threshold voltage or the point at which light is first generated; point B is the reverse breakdown voltage. This curve indicates that the LED is a low-impedance device similar to conventional silicon diodes, and it can be driven from low voltage supplies with conventional transistor circuitry. The wavelength of the LED's emitted light is nearly monochromatic as seen from the spectral curve of Figure 22. The light output of the LED will increase steadily with the current through it until a peak point is reached. Beyond this point the power output will decrease and the LED will be operating near

its maximum dissipation limit. Operation beyond this limit will result in junction heating and subsequent failure of the LED.

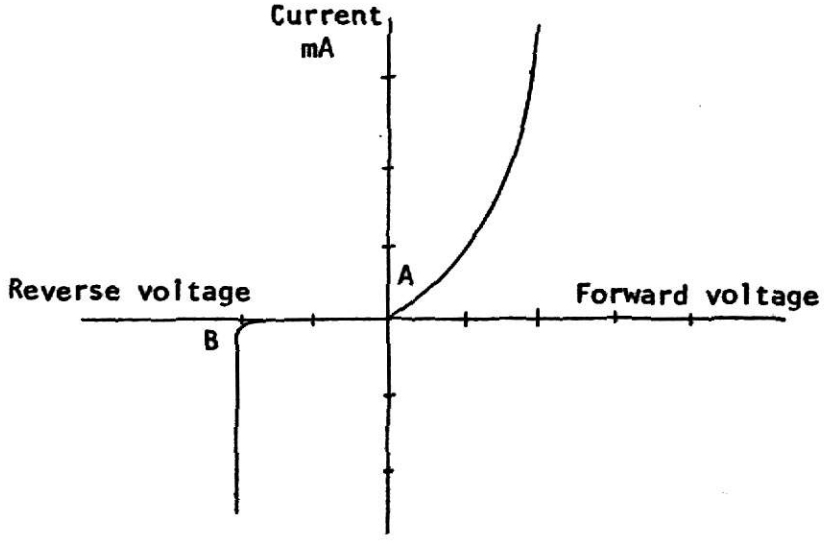

Fig. 21.--Typical LED curve

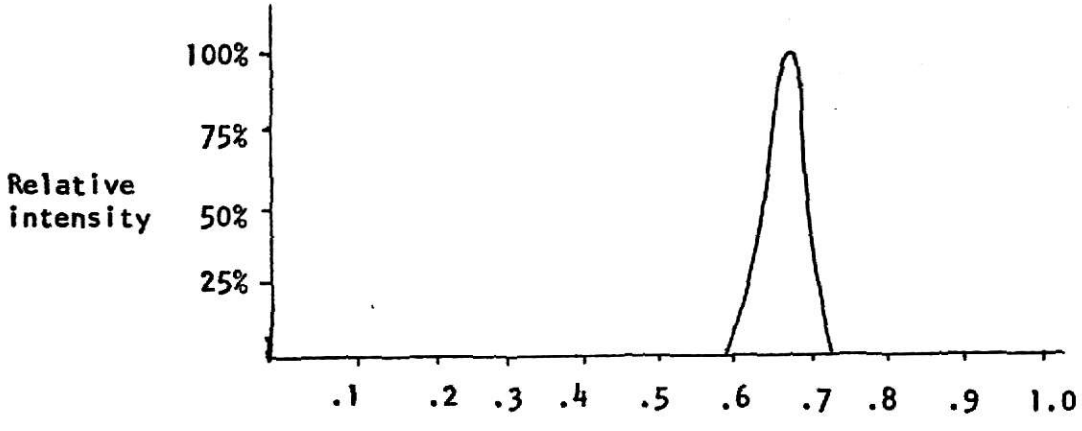

Fig. 22.--Spectral output of LED

The thermal properties of the LEDs are also of importance. The efficiency of a LED is a strong function of the operating temperature. A typical plot of the temperature variation of the output power normalized to room temperature is given in Figure 23. Since there is a decrease in output light

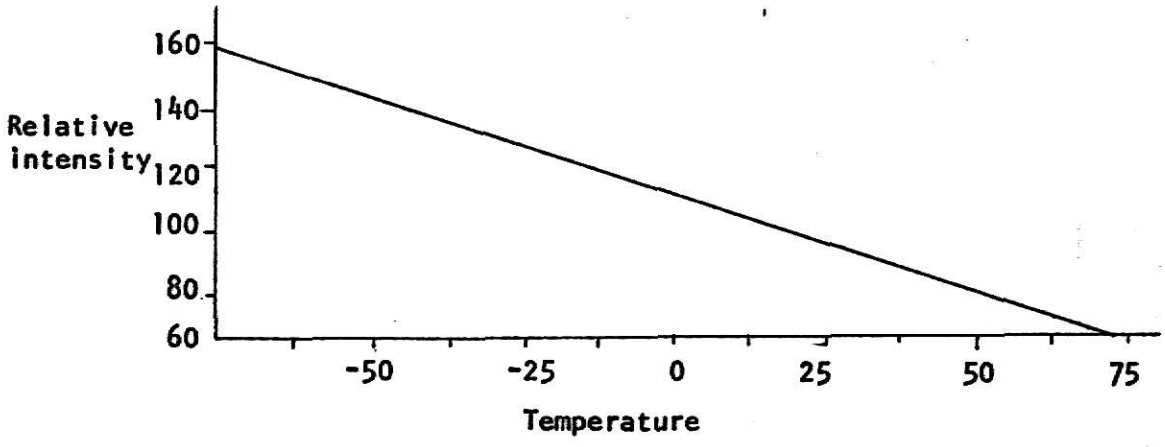

Fig. 23.--Temperature effect on output power

intensity with increasing temperature one must design with this in mind. The wavelength of peak emission decreases at a rate of 2 or 3 Angstroms per degree centigrade; however, if a wide spectral band receiving unit is used this will not affect transmission. Operating and storage temperature ranges of the LEDs are typically -65° C to 85° C with the upper temperature limit determined by the encapsulating material. By enclosing the LED in a portion of the head where the temperature will not exceed 50° C, the only temperature effect of importance will be the reduction of lamp intensity to 80% of its value at room temperature (25° C), as obtained from Figure 23.

A TIXL202 LED was chosen for this prototype circuit. The LED's parameters are included on data sheets (Appendix 1). The LED requires a maximum of 70 mA forward current, which is larger than the encoding circuit is capable of providing. Thus it is necessary to add an isolation stage followed by a medium power transistor capable of driving the LED into its light emitting state. This circuitry is shown in Figure 24. The output of the encoding circuit is a square wave of amplitude V_{cc} or V_{dd}, depending on the encoder state.

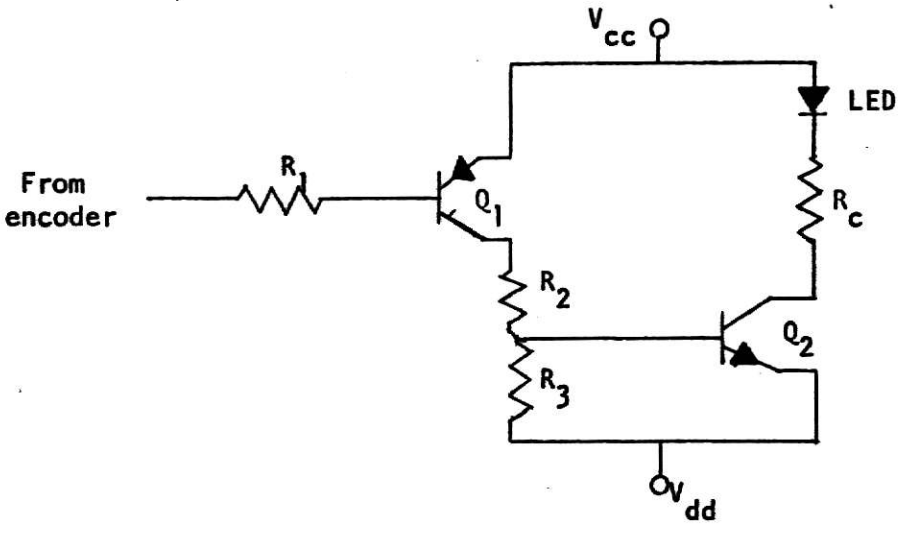

Fig. 24.--LED driver circuit

When it is in the V_{dd} state Q_2 of the driver circuit will be conducting and the LED will be forward biased. Thus there will be a visible light output with its intensity depending on the current I_p through it, where,

$$I_p = \frac{V_{cc} - V_{dd} - 1.5}{R_c}$$

and 1.5 is the voltage drop of the LED. When the encoder is in the V_{cc} state, Q_2 will be off and no current will flow through the LED; in this state there is no light emission. Since the encoder is a symmetrical circuit the duty cycle = $\frac{\text{time on}}{\text{period}}$ will be 1/2. Therefore, the average current I_{avg} through the LED will be 1/2 I_p. This average current must not exceed the 70 mA maximum rating to avoid damaging the diode.

The entire transmitting circuit for one channel of data is shown in Figure 25.

The Transmission Medium and Photodiode

As discussed earlier, the present telemetry system consists of 10 opti-

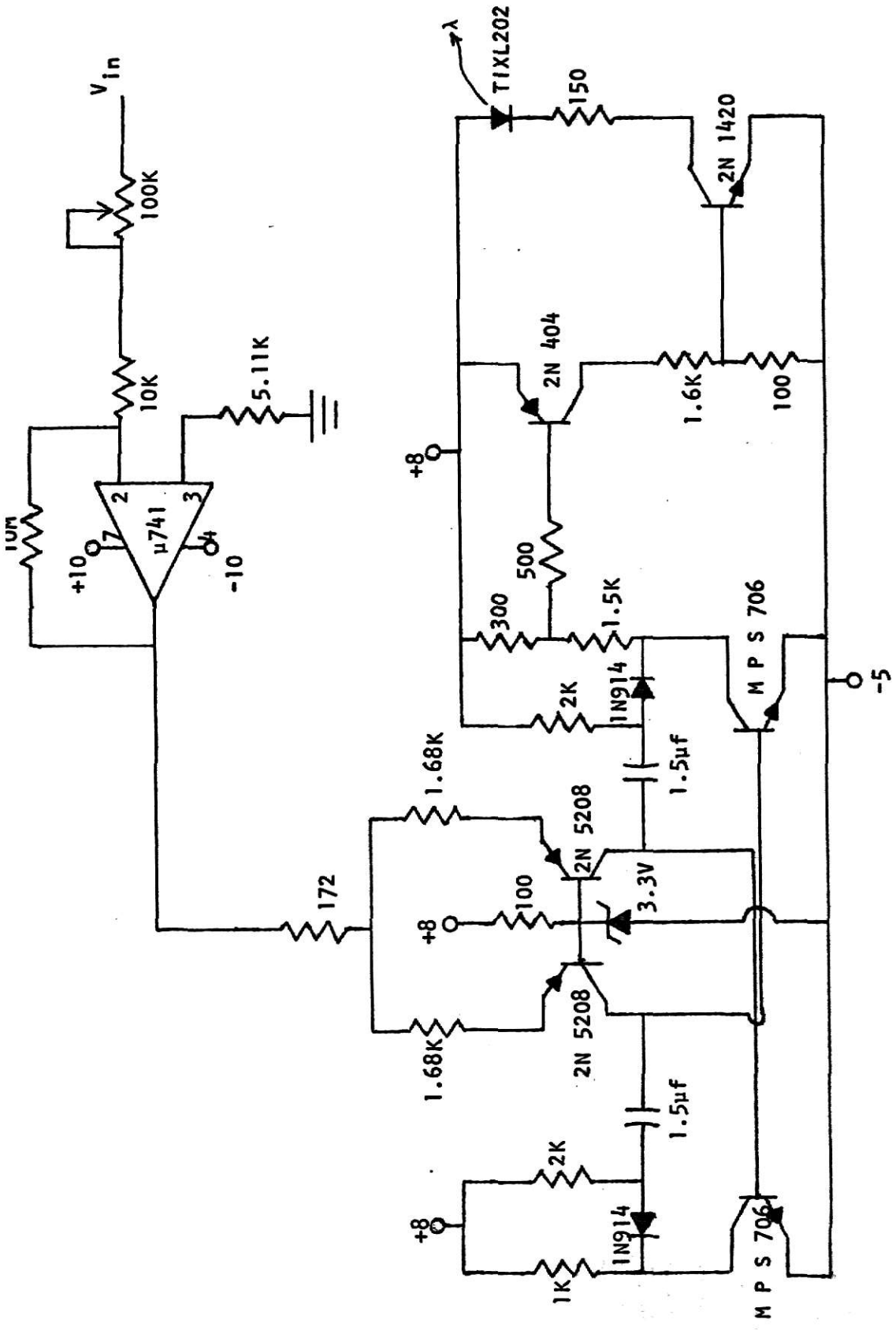

Fig. 25.--Transmitter

cally coupled channels. The argon bulb for each channel has a lens which focuses the light on a receiving lens above the photomultiplier tubes in the receiver. Each time an argon bulb, with typical life time of a few thousand hours, must be replaced, all ten channels must be removed and the alignment procedure must be carried out. The proposed system could use a lens also, but by using the plastic light fiber for the optical link, alignment will be essentially eliminated. The LED is fabricated with a lens to enhance light emission in a direction normal to the semiconductor chip. By treating the end of the light pipe with a finishing solution obtained from Edmund Scientific and holding the pipe in place perpendicular to the surface of the LED, maximum light will be incident on the pipe.

The light pipe used was obtained from Edmund Scientific and transmits light from 0.4 to 2 microns in wavelength. Twenty percent of the incident light is transmitted through 12 feet of the pipe, while 6 feet of the pipe will transmit forty-five percent of the incident light. A high voltage test on 1-1/2 inches of the light pipe indicated no current was observable up to 20,000 volts; at 30,000 volts 9 micro amperes was obtained. Since the length of the fiber optics pipe is 8 feet and the maximum voltage obtainable at the head is 600,000 volts, there should be no problem with surface current.

In any optoelectronic application the sensitivity of the available photodetectors at the particular emitted wavelength of the LED is just as important as the LED external efficiency. Detectors are generally inefficient at wavelengths emitted by narrow energy gap materials. Light sources emitting at wavelengths of one micron or less find a more favorable situation. Here photomultipliers, silicon photodiodes, photographic film or the human eye are very sensitive photodetectors. By comparing the emission spectra of the

solid state LEDs with the detector spectral response, the various LEDs can be matched to the detectors so as to give the highest coupling response. Figure 26 shows the spectral content of the LED above and different detectors below.

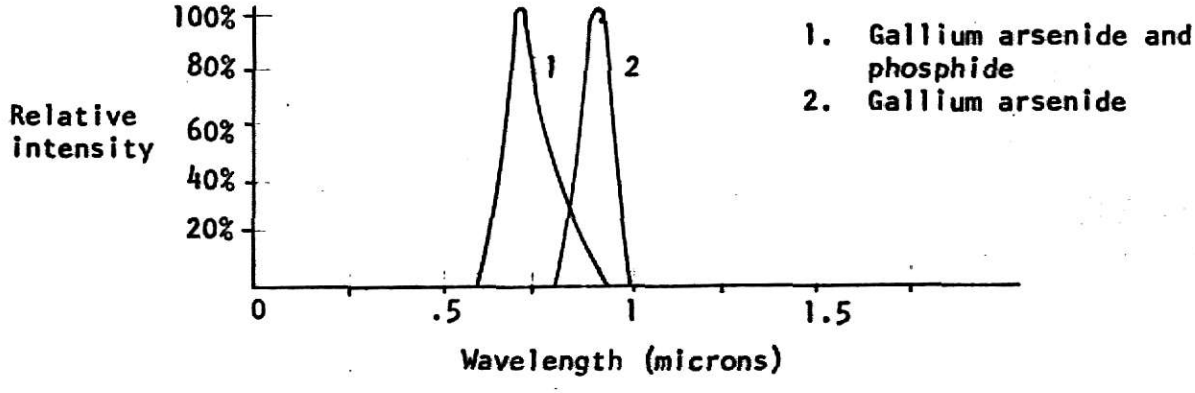

Spectral output of LED

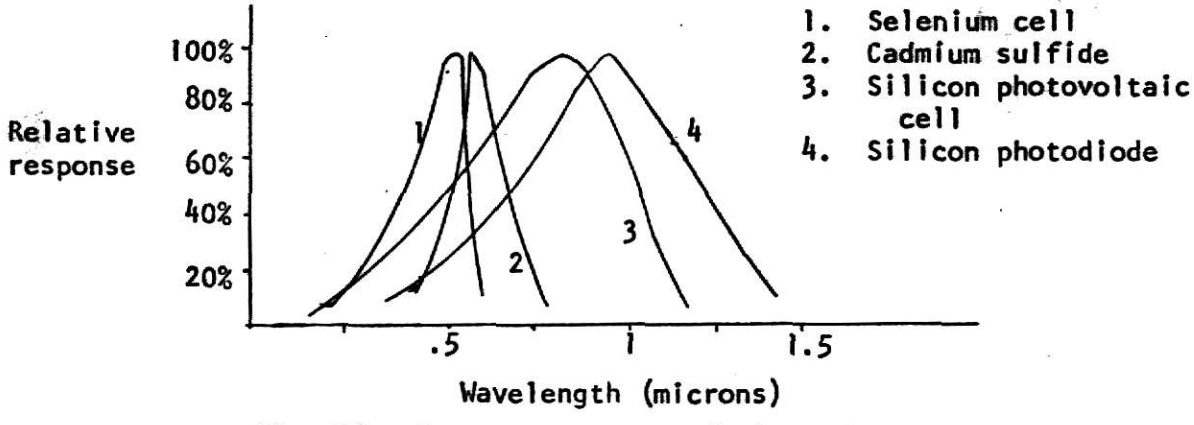

Fig. 26.--Response spectra of photo detectors

The gallium arsenide LED in combination with the silicon photodiode is one of the fastest switching optoelectronic combinations available. A TI LS 600 photodiode was chosen for the proposed circuit. The specifications are given in Appendix II.

The test circuit of Figure 27 was used to determine the attenuation effect of the light pipe for continuous light transmission. The results of this test are plotted on Graph 1. The solid curve is for air as the trans-

mission medium when the LED and photodiode are separated a distance of 1/4 inch, and the dotted line is for transmission through an 8 foot section of light pipe. As can be seen, the light fiber attenuates the signal considerably so that the output of the phototransistor is very low; a load resistor of 100 K is required to obtain a 2.3 mv signal.

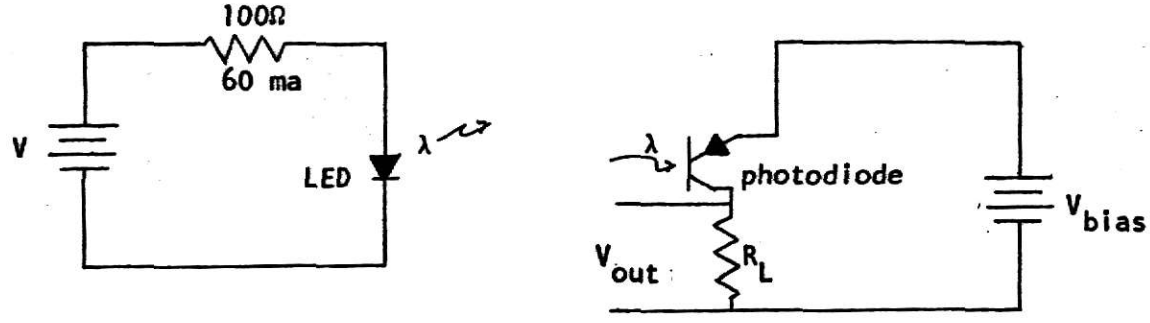

Fig. 27.--Test circuit

With a load resistor of 100 K another test was performed using a square-wave generator to drive the LED as in Figure 28.

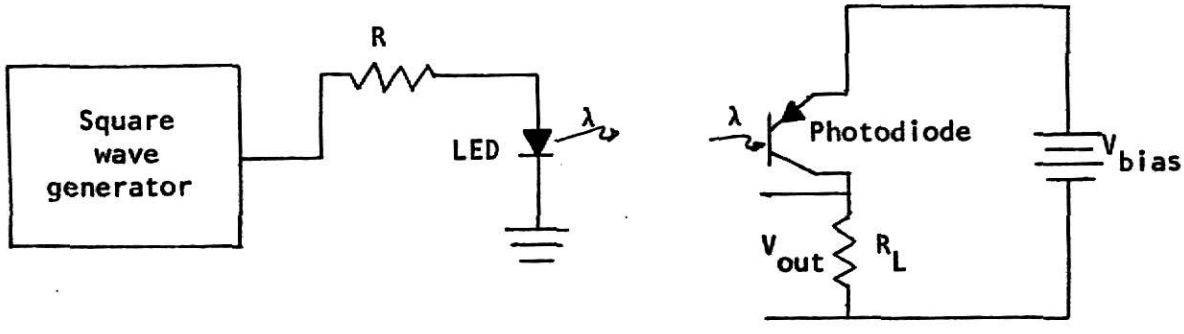

Fig. 28.--Waveform test circuit

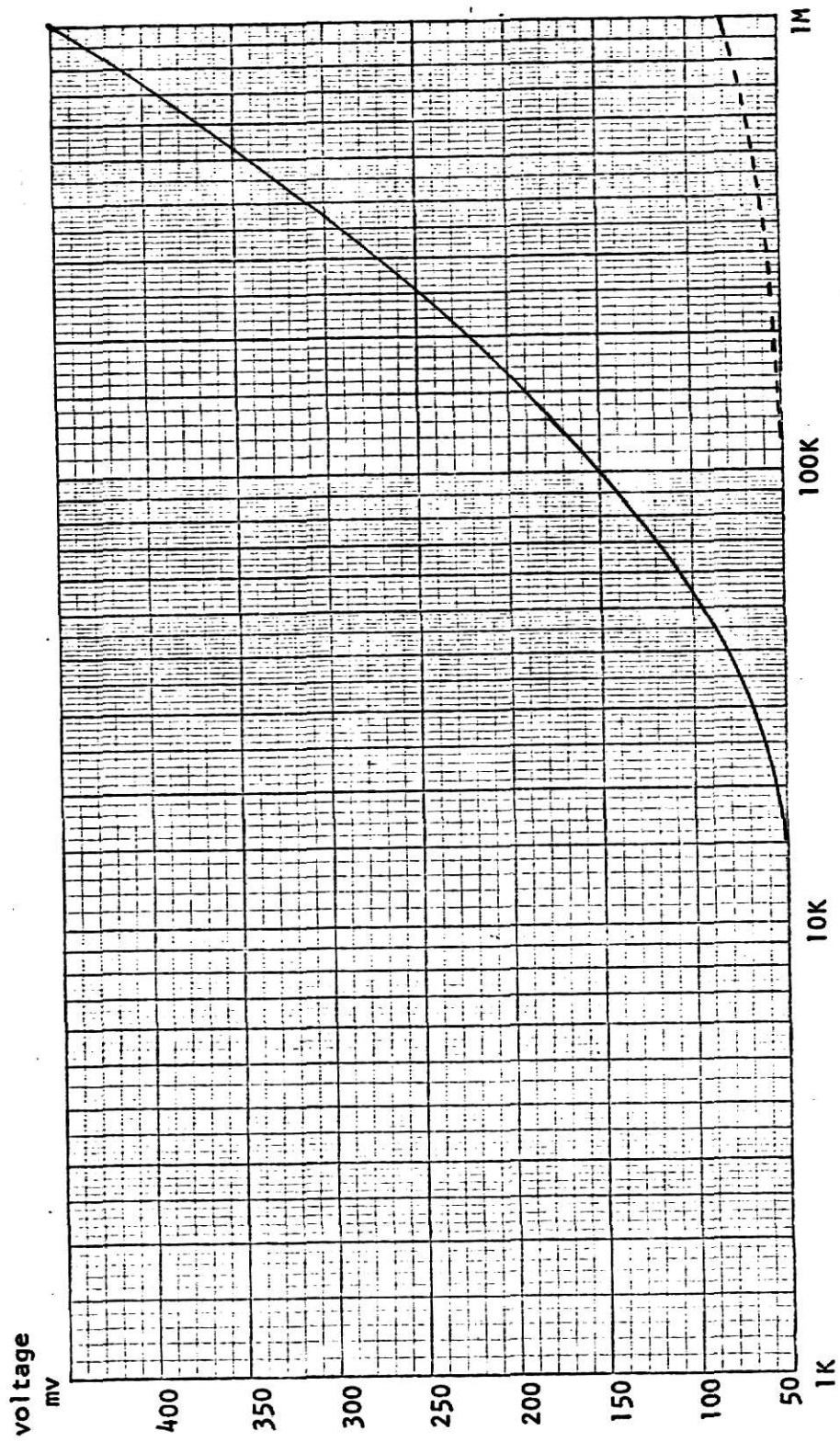
voltage
mv
400
350
300
250
200
150
100
50
1K
10K
100K
1M
Resistance R_L

Graph 1

The waveform V_{out} of the photodiode was fairly square up to 100 Hz, with easily distinguishable rise and fall points. At a frequency of 250 Hz the waveform is very poor, with no way of determining the turnon and turnoff point of the LED. Graph 2 shows the results. From these results the input impedance of the receiver should not exceed 100 K if the operating frequency of the transmitter is to be held to a maximum of 100 Hz.

Amplification and Shaping Circuit

The purpose of this section is to form the voltage of the photodiode into a voltage suitable for processing. Figure 29 is the amplifier and shaping circuit. The first operational amplifier takes the output of the photodiode and raises its value from a 2 mv maximum to a 200 mv value. This signal is used as the input of the second Op Amp which acts as a zero crossing detector. This Op Amp gives a fast rise and fall time square wave corresponding to the zero crossings of the input signal. The waveform at the

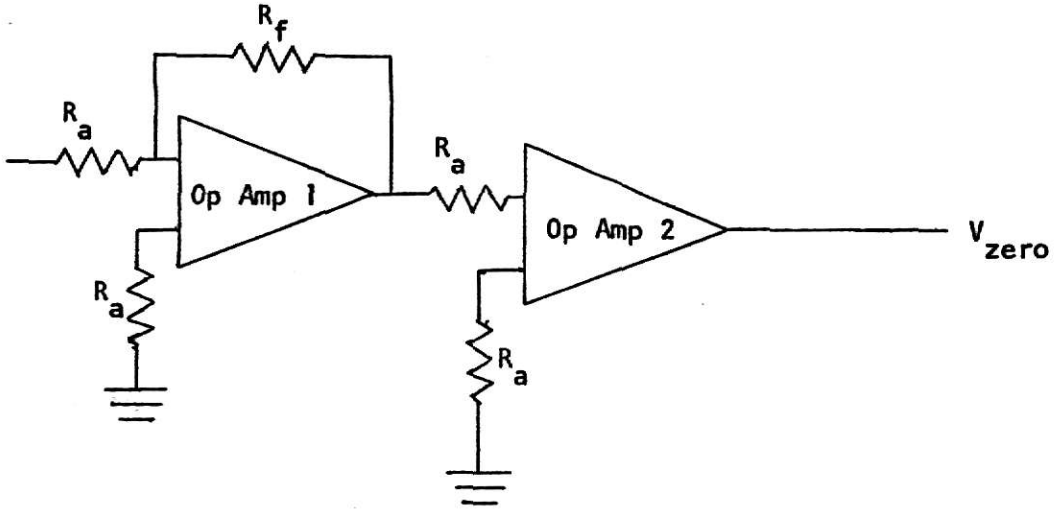

Fig. 29.--Amplifying and shaping circuit

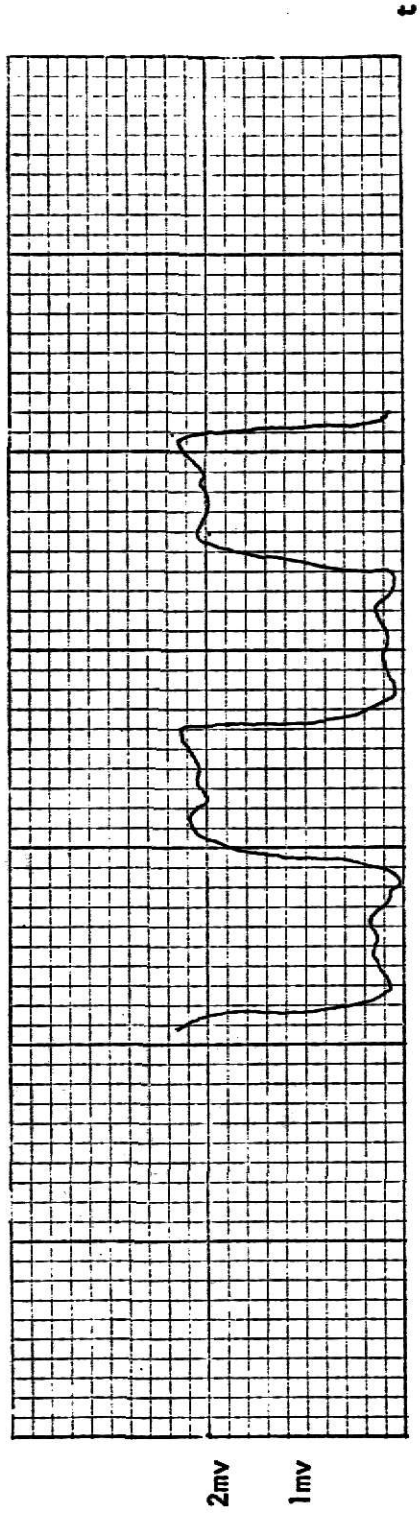

100 Hz signal

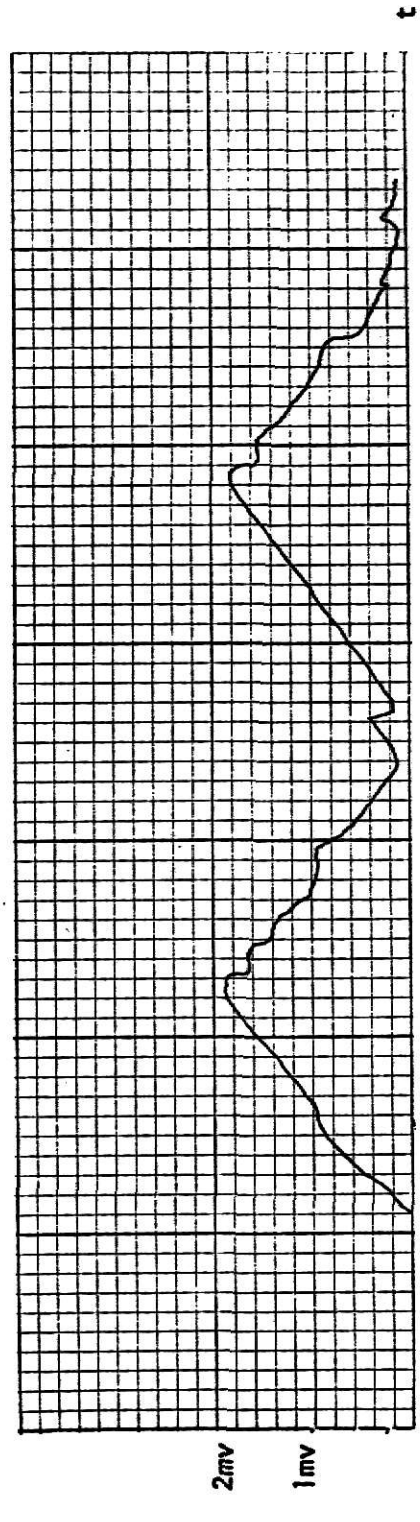

250 Hz signal

Graph 2

output of the second Op Amp is not a perfect square wave; however, this is not important. What is important is that it have the same frequency content as the transmitted waveform. This occurs when the zero crossings are detectable as in the 100 Hz signal of Graph 2.

Decoding Method and Circuit

The frequency variation of the waveform from the shaping section must now be transformed to a voltage without inducing any new errors. The method used in the proposed system is based on the same principle as the present system, i.e., taking a time average of pulses. To do this we must take the nearly square wave of the zero crossing detector output and form a pulse of given time duration for each negative going transition. The desired waveforms are indicated in Figure 30. The average voltage V_{avg} is then given by the following equation.

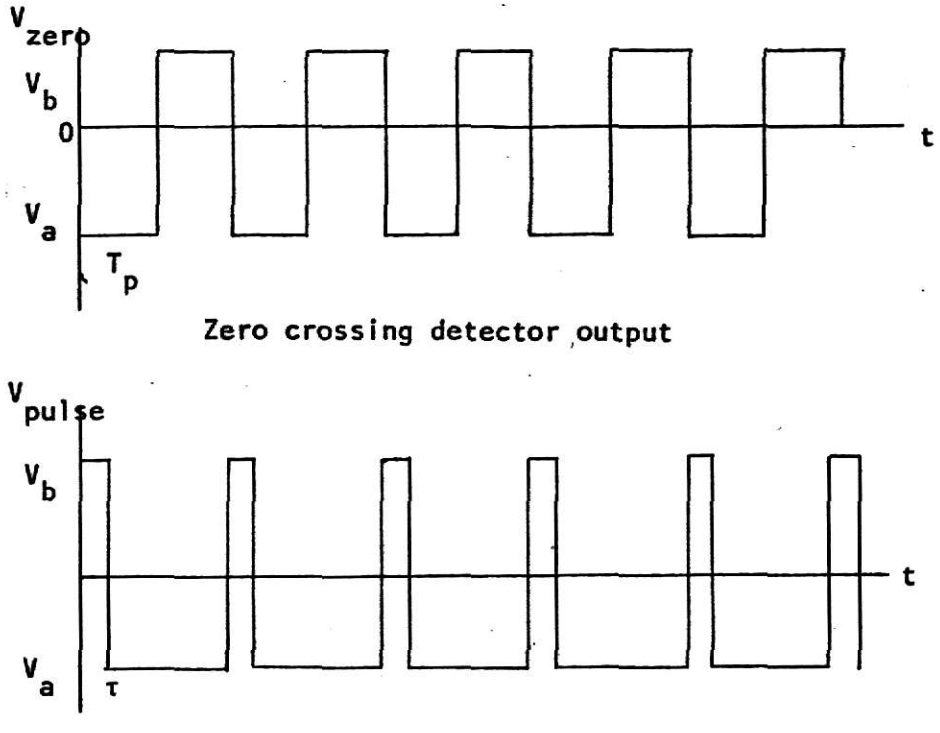

Fig. 30.--Fixed duration pulse output

$$V_{avg} = \frac{1}{T_p} \int_0^{\tau} E \, dt.$$

or,

$$V_{avg} = fE\tau,$$

where $f = \frac{1}{T_p}$ is the frequency of the encoder circuit.

The only requirement for linear decoding is that τ be independent of temperature. This can be achieved by building a monostable multivibrator from an Op Amp as in Figure 31. The value of τ is obtained by analyzing this circuit.

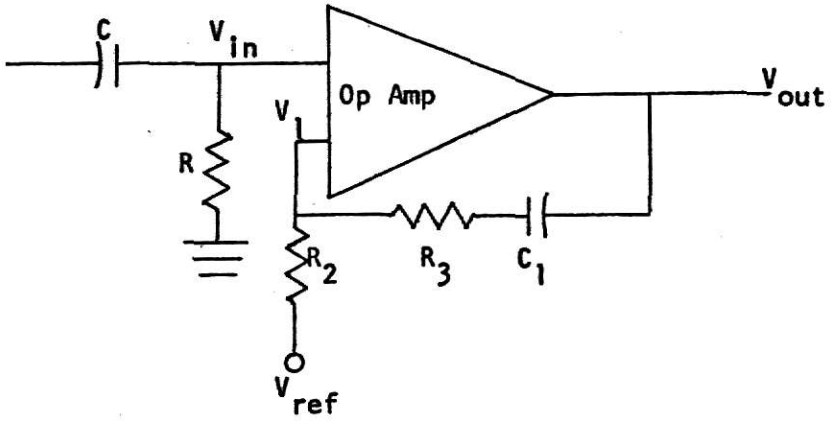

Fig. 31.--Monostable multivibrator

V_{ref} is at a negative potential so when V_{in} is zero V_{out} will remain negative. When V_{in} falls to a value below V_{ref} the output will jump to the positive value V_b. The output will remain positive until $V_1 = 0$, assuming that V_{in} has returned to zero prior to that time; at the time τ when $V_1 = 0$, the voltage will fall to its negative value V_a as in Figure 30.

Let the input pulse V_{in} occur at $t = 0$. We want to determine the time

τ it takes for V_1 in Figure 31 to return to zero. Drawing the circuit of the timing network with an initial condition generator for the capacitor, we have the circuit of Figure 32 just after t = 0.

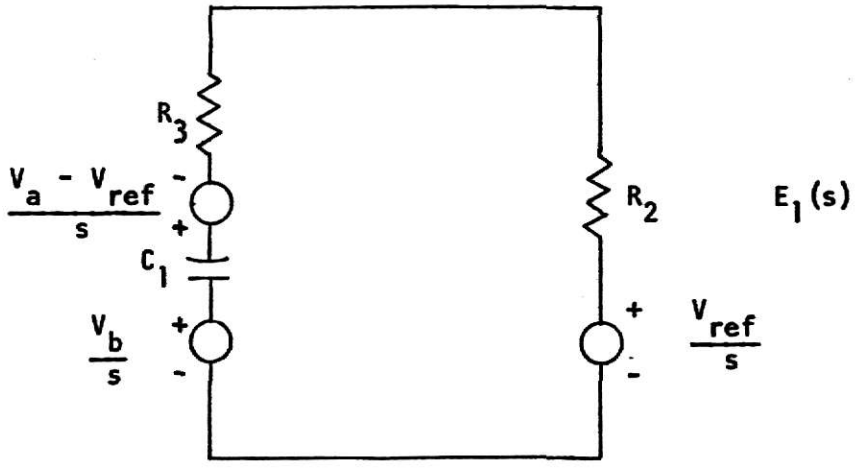

Fig. 32.--Timing circuit

Using superposition to obtain $E_1(s)$

$$E_1(s) = \frac{V_{ref}}{s} - \frac{R_2}{R_2 + R_3}\left(\frac{V_a - V_b}{s + \frac{1}{C_1(R_2 + R_3)}}\right) \tag{15}$$

Taking the inverse Laplace Transform of equation (15) produces

$$E_1(t) = V_{ref} - \frac{R_2}{R_2 + R_3}(V_a - V_b)\, e^{-\frac{t}{(R_2 + R_3)C_1}} .$$

We desire the value τ for $E_1(t) = 0$.

$$0 = V_{ref} - \frac{R_2}{R_2 + R_3}(V_a - V_b)\, e^{-\frac{\tau}{(R_2 + R_3)C_1}}$$

or

$$\tau = (R_2 + R_3)C_1 \ln \frac{\Delta V \, R_2}{V_{ref}(R_2 + R_3)} \tag{16}$$

where $\Delta V = V_a - V_b$.

The duration of the positive pulse is τ for every negative going pulse of the zero crossing circuit.

As was mentioned in the section explaining the encoder circuit, the lowest frequency obtainable is 10 Hz. Operation below this frequency would cause the meter needle to jump with each pulse. At 10 Hz there is still a small amount of oscillation of the meter, but it is not sufficient to impair the reading of the meter. One must, however, incorporate a method to zero the display unit. To accomplish this, an operational amplifier used as a difference amplifier follows the monostable multivibrator circuit. A reference voltage V_{ref} is added to the inverse of the multivibrator circuit, and this difference signal appears as the input to the ammeter. By adjusting the value of the reference voltage using R_0 to equal exactly the average value of the multivibrator output at 10 Hz, the ammeter will read zero at 10 Hz.

Figure 33 is the final receiver, decoding, and display circuit.

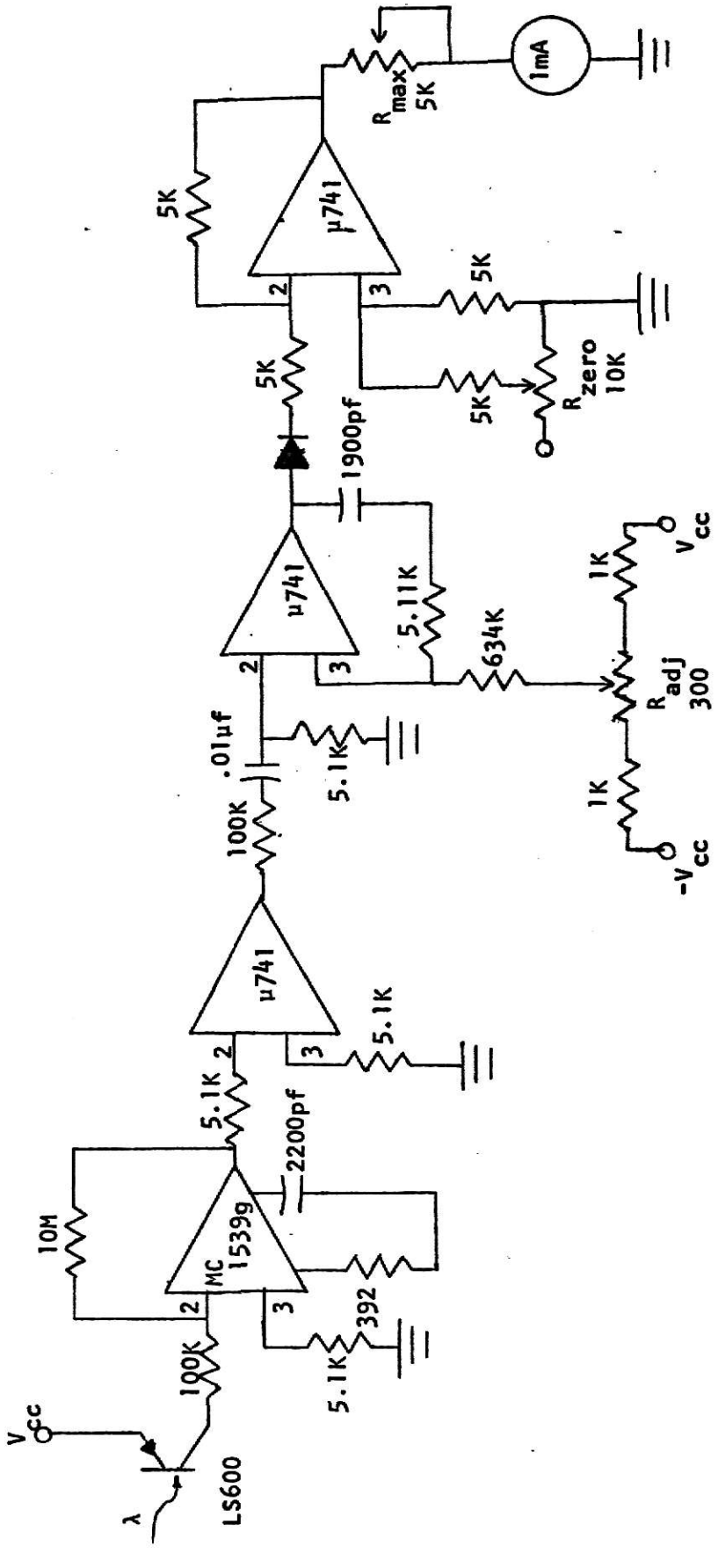

Fig. 33.--Receiver

CHAPTER IV

CONCLUSIONS AND SUGGESTIONS

Before discussing the accuracy of the proposed system, a few words on the adjustment and operation of the transmitter and receiver will be given. Some suggestions for further telemetry improvements will complete the paper.

There is one adjustment to be made on the transmitter circuit of Figure 25. All inputs will have a maximum value of V_{in} = 50 mv. Thus, each circuit with a 50 mv signal applied should be adjusted for a 110 Hz output signal. This adjustment is made by monitoring the output frequency using a frequency meter while the gain of the Op Amp is varied using R_g until the output frequency is 110 Hz. Next, setting V_{in} = 0, the frequency should drop to 10 Hz. The frequency need not be exactly 110 Hz or 10 Hz, but should not be more than ± 5 Hz from either value.

After treating both ends of the plastic light fiber with a capping solution, one end (transmitting end) is placed perpendicular to the LED, causing maximum incident light to be on the fiber. The other end is checked to make sure light is transmitted. The LED and transmitting end of the light fiber are properly aligned when the entire area of the receiving end of the light fiber has a red glow. The receiving end is then placed perpendicular to the photodiode at the Receiver of Figure 33. Now, if there is a square wave signal at the output of the shaping circuit, the plastic fiber and photodiode are properly aligned. With V_{in} = 50 mv for the receiver, the monostable multivibrator is adjusted for a nearly square wave output using R_{adj}. Next,

set V_{in} = 0 mv for the transmitter. The meter is adjusted to zero using R_{zero} in Figure 33. With V_{in} = 50 mv, the maximum setting or full scale reading is set using R_{max}.

Graph 3 is a plot of the proposed telemetry system output mA versus input mv. This linear relationship holds within 1% uncertainty.

There are two alternatives which should be considered for future improvements on the accuracy of this telemetry system. The first would use the same procedure with only a new encoder. The second is a new system which should be considered if a large number of channels of information are to be processed.

Since the start of this project the Signetic Corporation has introduced a voltage-to-frequency converter with stability on the order of 100 $\frac{ppm}{°C}$. This circuit requires one external resistor and one external capacitor for operation over a 10:1 frequency range, and is modulated over a similar 10:1 frequency range. This circuit should be investigated for use as the encoder circuit.

Secondly, one should investigate the possibility of using a time division multiplexing scheme. Figure 34 is a block diagram of such a scheme. It is assumed that there are n channels of data. The maximum number n depends on several factors including: frequency of the input data, sampling rate of the Analog-to-Digital (A/D) converter, and maximum speed of transmission. The accuracy of each sample depends on the A/D converter's accuracy. A timing circuit is included for synchronization of the switch and the A/D converter. The binary signal of the A/D converter is then transmitted via an optical channel, possibly using lenses to allow a higher frequency of operation in this case, to the photodiode. The signal is shaped, then displayed on a digital readout. Thus a binary to decade decoding circuit takes the place of a

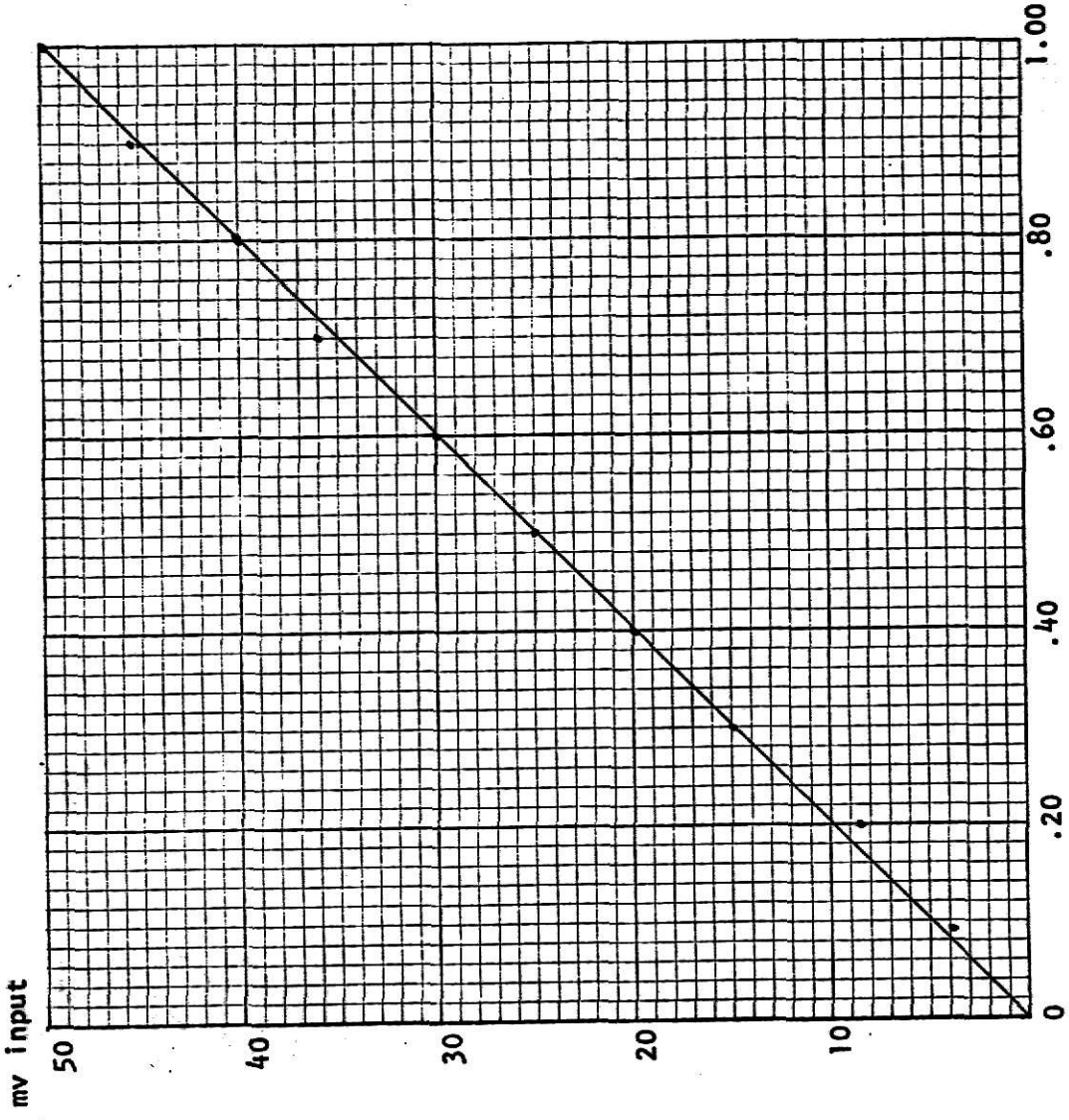

Graph 3

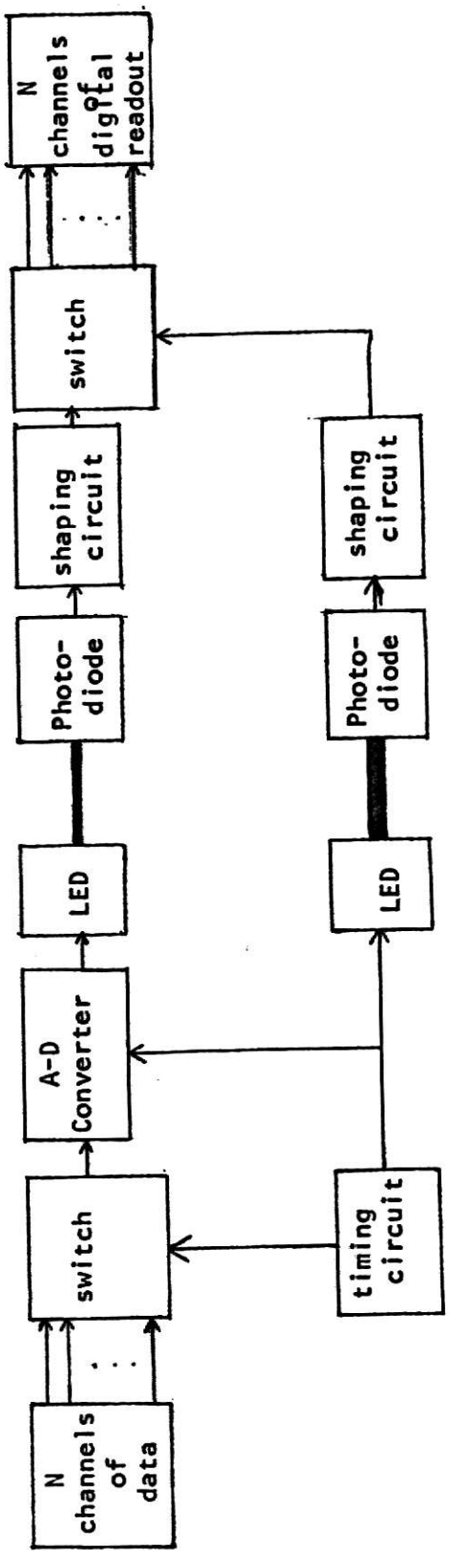

Fig. 34.--A suggested method

Digital-to-Analog converter. The timing circuit is optically coupled to a switch in the receiver allowing synchronization of the transmitted and displayed channels of data. One could include a magnetic tape storage unit to maintain a record of the parameter variations during any test that is conducted.

APPENDICES

APPENDIX I

TIXL202

Electrical Characteristics at 25° C Free Air Temperature

Parameter		Test Conditions	TIXL202			
			MIN	TYP	MAX	UNIT
peak	Wavelength at peak emission	I_f = 50 mA		6700		Å
BW_f	Spectral width between half power points	I_f = 50 mA		230		Å
θ	Emission beam angle between half power points	I_f = 50 mA		140		deg
V_f	Static forward voltage	I_f = 50 mA		1.9	3.0	V
C	Capacitance	V_f = 0, 1 MHz		135		pf
t_r	Rise time	I_f = 50 mA, 5 μ sec pulse		80		nSec
t_f	Fall time	40 KHz repetition rate		80		nSec
W_s	Brightness	I_f = 50 mA (see note 3)	100	400		ftL

Notes: 1. Derate linearly to 100° C free air temperature at the rate of 0.93 mA/°C.

2. Derate linearly to 100° C case temperature at the rate of 1.33 mA/°C.

3. Brightness is measured with a Gamma Scientific Brightness Spot Meter using a 0.011 inch spot focused on the brightest area of the emitting surface.

DATA TAKEN FROM TEXAS INSTRUMENTS Data Sheet

Absolute Maximum Ratings

Continuous forward current at (or below) 25° C free air temperature (see note 1)	70 mA
Continuous forward current at (or below) 25° C free air temperature (see note 2)	100 mA
Peak forward current (10 μ second pulse, 1 KHz)	2 A
Reverse voltage (reverse current 100 μA)	2 V
Operating case temperature range	55° C to 100° C
Storage temperature range	55° C to 100° C
Lead temperature ($\frac{1}{16}$ inch from case for 3 seconds)	200° C

APPENDIX II

LS600

Electrical Characteristics at 25° C Free Air Temperature

Parameter		Test Conditions	Min	Typ	Max	Unit
I_L	Light current	V_{ce} = 5V H = 20 mw/cm^2 (see note 1)	0.8	1.0		mA
I_D	Dark current	V_{ce} = 30V H = 0		0.01	0.025	µA
I_D	Dark current	V_{ce} = 30V H = 0 T_A = 100° C		10		µA
V_{ce} (sat)	Collector-emitter/ saturation voltage	I_L = 0.4 mA H = 20 mw/cm^2 (see note 1)		0.3		V

Note 1: Irradiance (H) is the radiant power per unit area incident upon a surface. For this measurement the source is an unfiltered Tungsten Filament Bulb operating at a 2870° K color temperature.

Switching Characteristics at 25° C Free Air Temperature

Parameter		Test Conditions	Typ	Min
t_r	Rise time	V_{ce} = 35V I_L = 800 µA	1.5	µ sec
t_f	Fall time	R_L = 1 KΩ	15	µ sec

DATA TAKEN FROM TEXAS INSTRUMENTS Data Sheet

Absolute Maximum Ratings at 25° C Free Air Temperature

Collector-emitter voltage . . . . . 50 V
Emitter-collector voltage . . . . . 7 V
Total device dissipation at (or below) 25° C free air temperature (see note 2). . . . . 50 mw
Operating free air temperature range . . . . . -65° C to 150° C
Storage temperature range . . . . . -65° C to 150° C
Soldering temperature (3 minutes) . . . . . 240° C

Note 2: Derate linearly to 125° C free air temperature at the rate of 0.5 mw/°C

SELECTED BIBLIOGRAPHY

Bell, E. C., and Robson, D. "Use of Multivibrators in Small Telemetry Systems." Proc. IEEE, Vol. 114, No. 3, March, 1967, 327-332.

Biddlecomb, R. W. "Latest Multivibrator Improvement, Linear Voltage-to-Frequency Converter." Electronics, April 26, 1963, 64-65.

Chew, J. R. "Multivibrator Design Difficulties." Wireless World, September, 1966, 465-467.

General Electric Glow Lamp Manual. General Electric Company, 1966.

Gruenberg, Elliot L. Handbook of Telemetry and Remote Control. New York: McGraw-Hill Book Co., 1967.

Hakim, S. S. Junction Transistor Circuit Analysis. New York: John Wiley & Sons, Inc., 1962.

Hertz, L. M. Solid State Lamps Part 1. General Electric Company, 1970.

Hurst, S. L., and Seal, C. L. "Frequency Control of Astable Transistor Multivibrator Circuits." Electronic Engineering, March, 1965, 182-185.

Meyers, R. S., and O'Brien, J. "Light-Emitting Diodes." Electronics World, July, 1969, 41-45.

Mims, Forrest M., III. "Light-emitting Diodes." Popular Electronics, November, 1970, 35-43.

Pepper, Clement S. "A Low-cost Constant-current Source." Radio Electronics, December, 1966, 62-64.

Rakovich, B. D., and Tesi, S. "Voltage to Frequency Conversion." Electronic Engineering, December, 1967, 766-768.

RCA Transistor Thyristor & Diode Manual. Radio Corporation of America, 1969.

Strauss, Leonard. Wave Generation and Shaping. New York: McGraw-Hill Book Co., 1970.

Tesic, S. "Simple Voltage-to-Frequency Converter with Increased Frequency Range." Electronic Engineering, March, 1969, 348-349.

TELEMETRY OF THE COCKCROFT-WALTON ACCELERATOR

by

JACK ROSS CRUMRINE

B. S., Kansas State University, 1969

AN ABSTRACT OF A MASTER'S REPORT

submitted in partial fulfillment of the

requirements for the degree

MASTER OF SCIENCE

Department of Electrical Engineering

KANSAS STATE UNIVERSITY
Manhattan, Kansas

1971

In any telemetry system there are three groups of equipment: a transmitter, transmission medium, and receiver. These three elements must be designed to yield the least amount of error in the transmission of data from a source of data to a remote point for human interpretation. The Cockcroft-Walton Accelerator operates at a potential of 600 KV above ground potential, necessitating a wireless telemetry system for monitoring different parameters located in the head. This paper investigates two methods of telemetry used to solve this problem. The first, termed the present system, was in use at Los Alamos. It consists of a relaxation oscillator optically coupled by lenses to a photomultiplier tube. The relaxation oscillator was designed using Argon Glow Lamps. Analysis of the operation of this circuit and the physical properties of glow lamps indicate that glow lamps operate very poorly as stable highly accurate voltage to frequency converters. Also, the use of lenses to optically couple the transmitter and receiver presents very difficult alignment problems. The second method, termed the proposed method, consists of a linear voltage controlled oscillator coupled to a LED for the transmitter. The LED is optically coupled to a photodiode by a plastic light fiber, essentially eliminating all alignment problems. The theory and practical problems of the voltage controlled oscillator are investigated, and a linear transmission of data is obtained.